Inter-symbol and Multi-user Interference Cancellation for LEO Satellite Systems

Felipe F. Souto, Victor Fernandes, Alberto G. Guimarães, Vinicius N. H. Silva and Roberto B. Di Renna

***Abstract*— The orthogonal time frequency space (OTFS) scheme has been considered a promising technique to deal with high Doppler scenarios, where inter-user and inter-symbol interference are significant. Studying the low Earth orbit (LEO) satellite systems, in this work we propose a DD multi-feedback successive interference cancellation (DD-MF-SIC) detector with shadow area constraints (SAC) to enhance symbol reliability and mitigate error propagation. A multi-user uplink scenario is considered, where users transmit over independent sparse delay–Doppler channels and the classical block linear minimum mean square error (BLMMSE) detector is used as a baseline. Simulation results show that the proposed approach yields relevant bit error rate (BER) gains under relevant Doppler conditions, with a competitive computational cost.**

***Keywords*— OTFS, detection, interference cancellation, LEO satellite channel.**

I. Introduction

As global connectivity requirements continue to increase, future communication networks are expected to look on Non-Terrestrial Networks (NTNs), particularly Low Earth Orbit (LEO) satellite constellations, to ensure ubiquitous coverage and full availability [1]. Although forecasts indicate that LEO systems will be crucial in the sixth generation of mobile communication systems (6G), they introduce significant communication limitations due to severe Doppler effects and very long propagation delays. To treat these high-mobility issues, Orthogonal Time Frequency Space (OTFS) scheme has been considered as a candidate technique. OTFS operates in the delay–Doppler domain, deals with channel diversity, and enhances resilience against fast time-varying channels, making it better adapted than conventional Orthogonal Frequency Division Multiplexing (OFDM) [2]. Recent studies have demonstrated that OTFS scheme has superior robustness compared to OFDM in LEO satellite systems, mostly under severe Doppler and multi-user interference conditions, where carrier frequency offsets (CFO) are relevant [3].

Although robust, signal detection in OTFS systems is challenging, especially in multi-user scenarios. Some authors have explored OTFS detection techniques to deal with channel particularities and to improve symbol treatment in high-mobility environments. Message Passing (MP) algorithm iteratively improves symbol estimates using probabilistic information, resulting in a relevant performance gain over OFDM [4], but without handling multi-user scenarios. Maximal Ratio Combining (MRC) detector proposed in [5] for point-to-point OTFS systems obtains low computational complexity. Despite the method demonstrating robust performance at LEO satellite communication systems under high Doppler conditions, it does not consider multi-user interference nor incorporate interference cancellation strategies. Minimum Mean Squared Error (MMSE) and Zero-Forcing (ZF) solutions have been used for multi-user scenarios, exploiting the specifications of the delay–Doppler channel matrix. Although these techniques properly work, they are not efficient for more than two transmit antennas [6].

While these methods provide valuable contributions, most do not study the impact of the multi-user and/or inter-symbol interference. To address this, we propose a Delay-Doppler Multi-Feedback Successive Interference Cancellation (DD-MF-SIC) scheme designed for multi-user OTFS systems to perform inter-symbol and multi-user interference cancellation. Drawing inspiration from a previously published approach [7], we design a detector that acts specifically on the Delay-Doppler domain, efficiently mitigating both multi-user and inter-symbol interference. This interference cancellation capability distinguishes our work from existing OTFS detection techniques and is particularly suited for LEO satellite communication scenarios. We studied the performance of our approach under Doppler conditions, delay spreads and OTFS frame configurations, following recent studies on multi-user OTFS scheme for LEO satellite systems [8], [9].

The remainder of this paper is organized as follows. Section II presents the system model with the fundamentals of the OTFS scheme. Section III details the proposed detection approach. Section IV provides simulation results and performance comparisons. Finally, conclusions are drawn in Section V.

II. System Model

A. OTFS transmission

The OTFS scheme is based on the delay–Doppler (DD) domain, which is related to the time–frequency (TF) domain by the symplectic finite Fourier transform (SFFT), a 2D discrete Fourier transform [2]. To aid comprehension, the transmission scheme is shown on the left side of Figure 1.

The DD grid, indexed by $m = 0, \ldots, M-1$ and $n = 0, \ldots, N-1$, can be represented as $\Gamma = \left\{ \left(\frac{m}{M\Delta f}, \frac{n}{NT} \right) \right\}$, where M and N represent the number of delay and Doppler bins, respectively. The delay and Doppler resolutions are $\frac{1}{M\Delta f}$ and $\frac{1}{NT}$, respectively, considering that the spacing between adjacent frequency components is $\Delta f = \frac{1}{T}$, where T is the duration of each OTFS block. We assume that the matrix $\mathbf{X} \in \mathbb{C}^{M \times N}$, denoted by $\mathbf{X}[m, n]$, composed of a modulation

Felipe F. Souto, PPGEET, Universidade Federal Fluminense (UFF), Niterói-RJ, e-mail: fsouto@id.uff.br; Victor Fernandes, Alberto G. Guimarães, Vinicius N. H. Silva and Roberto B. Di Renna, Departamento de Engenharia de Telecomunicações, Universidade Federal Fluminense (UFF), Niterói-RJ, e-mail: [fernandesvictor, agaspar, viniciusnhs, robertobrauer]@id.uff.br. This work was partially supported by Conselho Nacional de Desenvolvimento Científico e Tecnológico (CNPq) under grants 403784/2023-9, 402562/2024-0 and Fundação de Amparo à Pesquisa do Estado do Rio de Janeiro (FAPERJ) under grants E-26/200.667/2024, E-26/210.493/2024 and E-26/210.311/2024.

alphabet such as Quadrature Amplitude Modulation (QAM), are the DD samples on the grid Γ.

The DD samples $\mathbf{X}[m,n]$ are transformed into the time–frequency domain $\mathbf{Z}[l,k]$ using the inverse symplectic finite Fourier transform (ISFFT), defined as

$$\mathbf{Z}[l,k] = \frac{1}{\sqrt{NM}} \sum_{n=0}^{N-1} \sum_{m=0}^{M-1} \mathbf{X}[m,n]\, e^{j2\pi\left(\frac{nk}{N} - \frac{ml}{M}\right)}. \quad (1)$$

Note that the time–frequency grid is indexed by $l = 0,\ldots,M-1$ and $k = 0,\ldots,N-1$. Therefore, the resulting matrix $\mathbf{Z} \in \mathbb{C}^{M\times N}$ contains the modulated time–frequency symbols to be transmitted.

In the next step, the Heisenberg transform maps the two-dimensional time–frequency samples $\mathbf{Z}[l,k]$ into a continuous-time waveform $s(t)$ using a transmit pulse $g_{\text{tx}}(t)$. The resulting transmitted signal is expressed as

$$s(t) = \sum_{k=0}^{N-1} \sum_{l=0}^{M-1} \mathbf{Z}[l,k]\, g_{\text{tx}}(t-kT)\, e^{j2\pi l\Delta f(t-kT)}. \quad (2)$$

B. Channel

The continuous-time signal $s(t)$ goes through a time-varying channel characterized by the DD response $h(\tau,\nu)$, where τ and ν are the delay and Doppler shift of the channel, respectively, and is modeled as

$$h(\tau,\nu) = \sum_{q=1}^{P} h_q\, \delta(\tau-\tau_q)\, \delta(\nu-\nu_q), \quad (3)$$

where P is the total number of multipath components, h_q represents the complex channel coefficients of the q-th path, while τ_q and ν_q correspond to the delay and Doppler shift of the q-th path, respectively.

The total Doppler shift experienced at the receiver is expressed as

$$f_d = f_{\text{sat}} + f_c\, \frac{v_u}{c} \cos\alpha, \quad (4)$$

where f_{sat} is the Doppler shift due to the satellite motion, f_c is the carrier frequency, v_u is the user velocity, c is the speed of light, and α is the elevation angle between the user and the satellite. The Doppler shift due to satellite motion is given by

$$f_{\text{sat}} = \frac{f_c}{c}\, v_{\text{sat}} \left(\frac{R}{R+h}\, \cos\alpha\right), \quad (5)$$

where v_{sat} is the satellite velocity, R is the Earth's radius, and h is the satellite altitude. This Doppler shift is assumed to affect all channel taps uniformly.

C. OTFS reception

The received signal $r(t)$ resulting from transmission through a time-varying channel can be represented in the DD domain as

$$r(t) = \iint h(\tau,\nu)\, s(t-\tau)\, e^{j2\pi\nu(t-\tau)}\, d\tau\, d\nu \quad (6)$$

At the receiver, the received signal $r(t)$ passes through a matched filter $g_{\text{rx}}(t)$, resulting in the cross-ambiguity function

$$Z(f,t) = A_{g_{\text{rx}},r}(f,t) \triangleq \int r(t')\, g_{\text{rx}}^{*}(t'-t)\, e^{-j2\pi f(t'-t)}\, dt', \quad (7)$$

where $(\cdot)^*$ denotes the complex conjugate. Sampling this function over the grid $f = l\Delta f$, $t = kT$ produces the time-frequency domain received matrix $\boldsymbol{\mathcal{Z}}[l,k] \in \mathbb{C}^{M\times N}$, given by

$$\boldsymbol{\mathcal{Z}}[l,k] = Z(f,t)\Big|_{f=l\Delta f,\, t=kT}, \quad (8)$$

which is referred to as the Wigner transform of the received signal [2].

Next, the symplectic finite Fourier transform (SFFT), consisting of an M-point inverse DFT across the columns and an N-point DFT across the rows of $\boldsymbol{\mathcal{Z}}[l,k]$, is applied to obtain the received samples in the DD domain. This results in the DD domain matrix $\mathbf{Y} \in \mathbb{C}^{M\times N}$ given by

$$\mathbf{Y}[m,n] = \frac{1}{\sqrt{MN}} \sum_{k=0}^{N-1} \sum_{l=0}^{M-1} \boldsymbol{\mathcal{Z}}_{\text{tf}}[l,k]\, e^{-j2\pi\left(\frac{nk}{N} - \frac{ml}{M}\right)}. \quad (9)$$

III. Detection Techniques

This section presents the proposed algorithm, the DD Multi-Feedback Successive Interference Cancellation (DD-MF-SIC). Since DD-MF-SIC is an interference cancellation technique based on MMSE, the Block Linear MMSE (BLMMSE) approach will first be presented and used as an upper bound in the simulations. Let U denote the number of users transmitting simultaneously. The uncoded OTFS block diagram that illustrates the entire process of DD-MF-SIC is shown in Figure 1. After the SFFT, the receiver obtains a DD domain matrix $\mathbf{Y} \in \mathbb{C}^{M\times N}$, which contains the contributions of all users. This matrix is reshaped into a column vector $\mathbf{y} \in \mathbb{C}^{MN\times 1}$, which is modeled as

$$\mathbf{y} = \sum_{u=1}^{U} \mathbf{H}_u \mathbf{x}_u + \mathbf{n}, \quad (10)$$

where $\mathbf{x}_u \in \mathbb{C}^{MN\times 1}$ is the vectorized version of the transmitted symbols of the user u, $\mathbf{H}_u \in \mathbb{C}^{MN\times MN}$ is the equivalent channel matrix in the DD domain for that user, and $\mathbf{n} \sim \mathcal{CN}(0,\sigma_n^2)$ represents the additive white Gaussian noise. This representation, employing vectorized elements, is used as a model for detection explanation.

A. Block Linear MMSE (BLMMSE) Detection

The BLMMSE detector jointly estimates all users symbols by applying a linear filter that minimizes the mean square error. The global transmit vector is composed by concatenating the symbol vectors of all users: $\underline{\mathbf{x}} = [\mathbf{x}_1,\cdots,\mathbf{x}_U]^{\text{T}} \in \mathbb{C}^{UMN\times 1}$ and the overall multiuser channel matrix is

$$\underline{\mathbf{H}} = [\mathbf{H}_1\mathbf{H}_2\cdots\mathbf{H}_U] \in \mathbb{C}^{MN\times UMN}.$$

Considering all symbols have the same energy, the BLMMSE estimate of the transmitted vector is computed as $\hat{\underline{\mathbf{x}}} = \left(\underline{\mathbf{H}}^{\text{H}}\underline{\mathbf{H}} + \sigma_n^2\mathbf{I}\right)^{-1}\underline{\mathbf{H}}^{\text{H}}\underline{\mathbf{y}}$, where σ_n^2 is the noise variance. Each estimated symbol is then assigned to the nearest constellation point using a hard-decision slicer. We also consider that $(\cdot)^{\text{H}}$ denotes the Hermitian operator and $\mathbf{I}$ is the identity matrix.

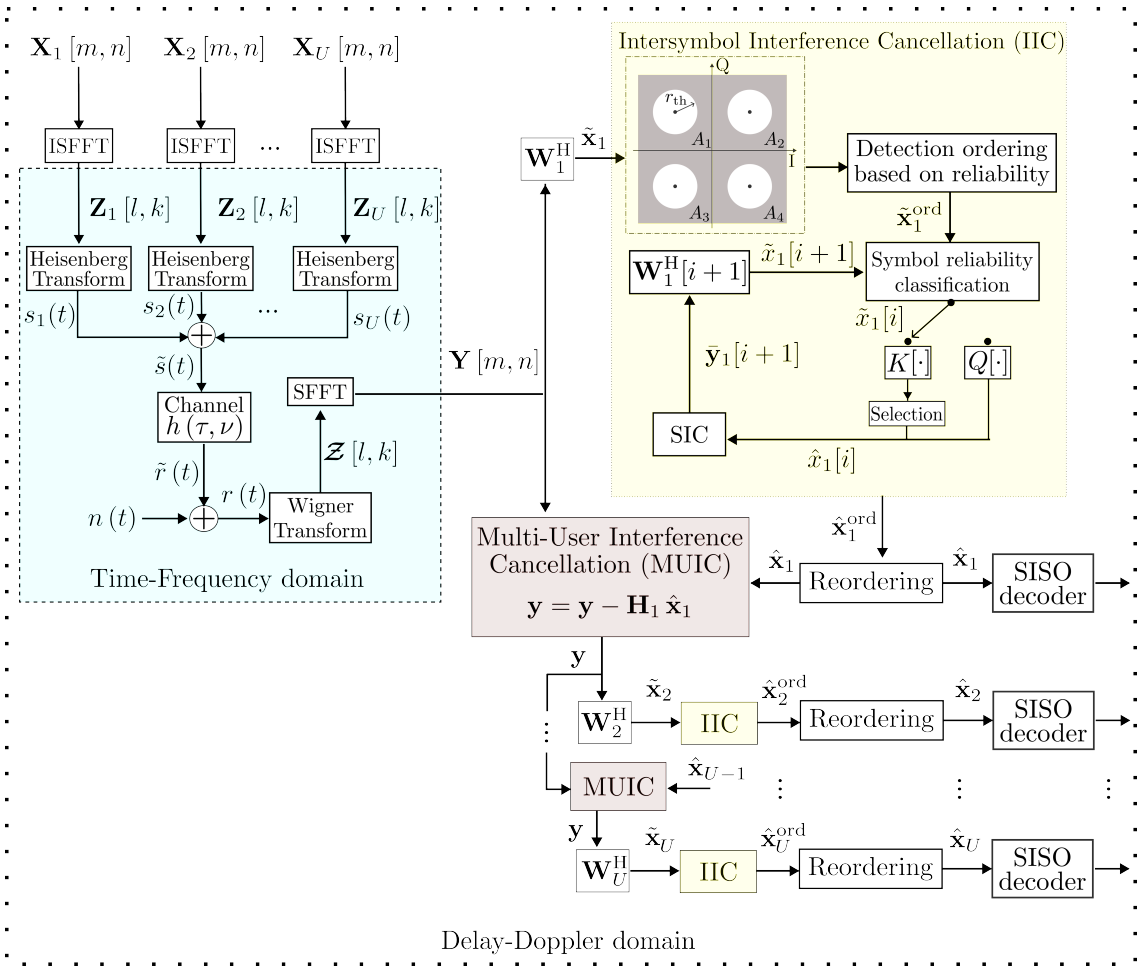

Fig. 1: Multi-user OTFS scheme with DD-MF-SIC detection.

B. Proposed Delay-Doppler Multi-Feedback Successive Interference Cancellation (DD-MF-SIC)

The contribution can be divided into two parts: Inter-Symbol Interference Cancellation (IIC) and Multi-User Interference Cancellation (MUIC). First, the receiver determines the user detection order using a well-known metric to perform Successive Interference Cancellation (SIC). Once the user is selected for detection, the IIC process begins. The IIC procedure relies on the reliability of the soft estimates of the user's symbols. The detector computes the soft estimates symbol by symbol and evaluates their reliability using a method known as the Shadow Area Constraint (SAC). If the i-th symbol falls within the SAC region, it is considered unreliable and is added to a list. After all frame symbols have been checked, the entries in the IIC list are sorted from the most to the least unreliable. The idea is to cancel the interference from the unreliable soft estimates first. Following this classification, the algorithm proceeds with steps similar to those of MF-SIC [10]. The received vector $\mathbf{y}$ is updated by removing the influence of the previously detected symbol. Once the entire frame has been detected, the IIC process ends. Before starting the detection of the next user's frame, the final version of the detected vector of the u-th user is used to cancel the multi-user interference, as is done in conventional SIC.

1) Inter-symbol Interference Cancellation: The DD-MF-SIC evaluates the reliability of soft estimates using a *shadow area constraint* (SAC), comparing the soft symbol estimate with all elements of a constellation alphabet [10], as represented in Fig. 1. For each user u, the i-th soft MMSE estimate is $\tilde{x}_u[i] = \mathbf{W}_u^{\mathrm{H}}[i]\mathbf{y}$, where

$$\mathbf{W}_u^{\mathrm{H}}[i] = \left(\mathbf{H}_u^{\mathrm{H}}[i]\mathbf{H}_u[i] + \sigma_n^2\mathbf{I}\right)^{-1}\mathbf{H}_u[i], \tag{11}$$

where $\mathbf{y}$ is the current residual received vector. Next, the SAC obtains this soft estimate and computes a distance metric as

$$r = \min_{i\in\{1,\ldots,|\mathcal{A}|\}} \|\mathcal{A}_i - \tilde{x}_u[i]\|, \tag{12}$$

where $\mathcal{A}$ is the modulation alphabet. If the reliability test fails (that is, $r > r^{\text{th}}$), where r_{th} is the SAC radius threshold, the estimate is considered unreliable and is added to an internal list for detection ordering. After all frame symbols have been evaluated, the entries in the IIC list are sorted from the least to the most reliable. To complete the list with all frame symbols, the so-called reliable symbols remain in their original positions, following the list of unreliable ones.

Following the IIC list order, the DD-MF-SIC proceeds as the traditional MF-SIC. If the soft estimate was previously considered reliable (that is, $r < r^{\text{th}}$), it is quantized to the closest symbol in $\mathcal{A}$, as

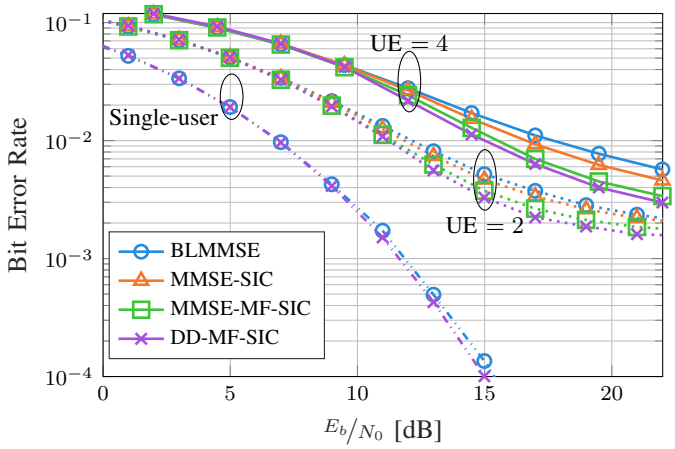

Fig. 2: Detection techniques comparison, $M = N = 32$, 1000 Monte Carlo iterations.

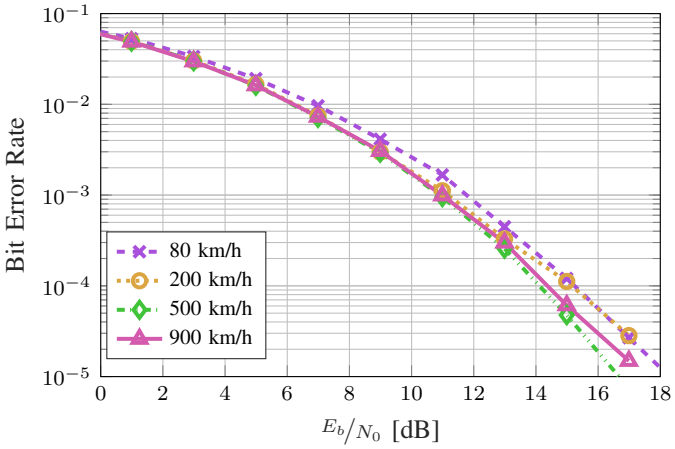

Fig. 3: DD-MF-SIC under single-user scenario for different velocities, $M = N = 32$, 1000 Monte Carlo iterations.

$$\hat{x}_u[i] = Q\left(\mathbf{W}_u^{\mathrm{H}}[i]\,\mathbf{y}[i]\right), \tag{13}$$

and the interference is canceled using:

$$\mathbf{y}_u[i+1] = \mathbf{y}_u[i] - \mathbf{h}_u[i]\hat{x}_u[i]. \tag{14}$$

If the reliability check failed, a list of candidates $K = \{K_1, \ldots, K_{|\mathcal{A}|}\} \subseteq \mathcal{A}$ is formed. The optimal candidate is then selected according to the minimum Euclidean distance:

$$K_{\text{opt}} = \arg \min_{j \in \{1,\ldots,|\mathcal{A}|\}} \|\mathbf{y}[i] - \mathbf{h}_u[i]K_j\|. \tag{15}$$

After choosing the optimal candidate, K_{opt} occupies the place of $\hat{x}_u[i]$ and DD-MF-SIC proceeds to the $i+1$-th symbol. When all the symbols are detected, the next step is the multi-user interference cancellation.

2) Multi-user Interference Cancellation: The MUIC part improves linear detection using interference cancellation. The users are detected sequentially, following the order previously established, and after each detection, the estimated signal of the user is subtracted from the received vector before proceeding to the next one. The steps are similar to the IIC, but without the reliability test and the candidates list. DD-MF-SIC cancels the interference of the i-th user, as in (14), but considered the whole frame, as $\mathbf{y}_{u+1} = \mathbf{y}_u - \mathbf{H}_u\hat{\mathbf{x}}_u$, where $\mathbf{y}_{u+1}$ indicates that the received vector $\mathbf{y}$ is updated by the interference cancellation process. This process is repeated until the last user.

IV. Simulation Results

To verify the performance of the proposed algorithm, we consider a multiuser uplink system operating over a DD grid with $N = 32$ Doppler bins and $M = 32$ delay bins, using 4-QAM modulation. The system is a multi-input-single-output system, thus one can consider that the satellite has only one antenna. The idea is to check the influence of the interference in the transmissions. The main simulation parameters are summarized in Table I. Throughout the simulation, the elevation angle did not change. The satellite channel model follows the 3GPP NTN-TDL-B profile [11] with Rayleigh fading and four normalized taps. The normalized delay and power profile used are detailed in Table II.

TABLE I: Simulation Parameters for LEO Satellite Scenario.

Parameter	Value
Subcarrier spacing (Δf)	30 kHz
Carrier frequency (f_c)	40 GHz
Satellite velocity (v_{sat})	7.11 km/s
Satellite altitude (h)	1500 km
Earth radius (R)	6371 km
Elevation angle (α)	10°

The real delay of each tap is obtained by multiplying the normalized delay values by a desired RMS delay spread $\tau_{q,\text{scaled}} = \tau_{q,\text{model}} \cdot \text{DS}_{\text{desired}}$, where $\text{DS}_{\text{desired}}$ is the RMS delay spread [12], set in this work to 1000 ns.

Figure 2 presents the BER performance as a function of Eb/N_0 for scenarios with a single user, two users, and four users, comparing the detection techniques. The user speed was set to 80 km/h and the SAC radius thresholds r_{th} was set to 1.0. The DD-MF-SIC detector demonstrates superior robustness to interference caused by additional users, performing better in terms of inter-symbol and multi-user interference mitigation.

Figure 3 illustrates the performance of an OTFS single-user varying the velocities using our proposed approach. The user speeds range from 80 km/h to 900 km/h. The SAC radius thresholds r_{th} was set to 1.0. It is observed that the BER performance improves as the user speed increases, as does the Doppler spread. This can be explained by the fact that the Doppler spread becomes larger than the Doppler resolution, resulting in a better separation of multipath components in the DD grid. However, when the speed is set above 500 km/h, all paths become more distinguishable by having different delay and Doppler bins. Hence, Doppler spread saturation offers limited additional benefits [2].

Figure 4 presents the performance of the system under different SAC radius thresholds r_{th} and the number of users. The simulations were performed varying the thresholds r_{th} into a specific set of ten values considering both the single-user scenario, Figure 4 (a), and the three-users scenario, Figure 4 (b). Through this analysis, it was possible to verify the optimal values of r_{th} for each scenario, shown in Table III, demonstrating that there is a room of improvement of using these optimal values to improve performance according to the scenario configuration.

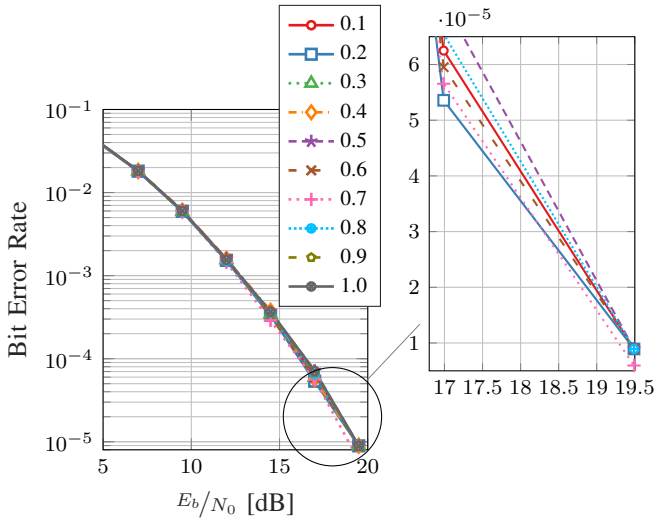

(a) Single-user scenario.

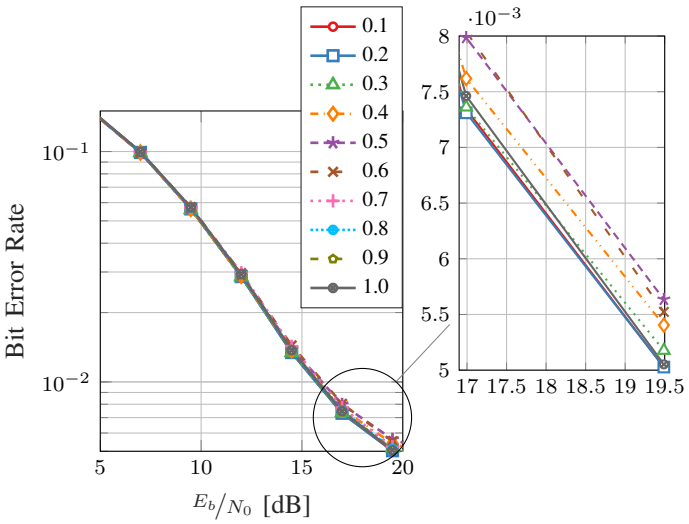

(b) Zoom in UE= 3 scenario.

Fig. 4: BER vs. E_b/N_0 for DD-MF-SIC under different SAC radius thresholds.

TABLE II: Parameters for LEO Satcom System.

Tap	Normalized delay	Power [dB]	Fading
1	0.0000	0.000	Rayleigh
2	0.7249	-1.973	Rayleigh
3	0.7410	-4.332	Rayleigh
4	5.7392	-11.914	Rayleigh

TABLE III: Optimal r_{th} values for different E_b/N_0 level.

E_b/N_0 [dB]	r_{th} (UE=1)	r_{th} (UE=3)
2	0.4	0.6
4.5	0.3	0.5
7	0.7	0.4
9.5	0.8	0.3
12	0.7	0.3
14.5	0.7	0.3
17	0.2	0.2
19.5	0.7	0.1

V. Conclusion

This work evaluated the performance of different detection techniques for multi-user OTFS scheme in LEO satellite communication systems, characterized by high Doppler and delay dispersion. The proposed DD-MF-SIC enhances detection robustness by introducing a reliability check and exploring multiple candidate decisions based on reliability. Simulation results demonstrate that DD-MF-SIC achieves superior BER performance, especially under high interference conditions, making it a promising approach to multi-user detection in LEO satellite OTFS systems. As future work, the proposed detection scheme can be extended to MIMO-OTFS scenarios. Furthermore, dynamically adjusting the SAC radius thresholds based on the estimated Doppler spread or E_b/N_0 values may further improve the detection accuracy by adapting the reliability region to varying channel conditions.

Acknowledgements

This work was partially supported by Conselho Nacional de Desenvolvimento Científico e Tecnológico (CNPq) under grants 403784/2023-9, 402562/2024-0 and Fundação de Amparo à Pesquisa do Estado do Rio de Janeiro (FAPERJ) under grants E-26/200.667/2024, E-26/210.493/2024 and E-26/210.311/2024.

References

[1] Samsung Electronics, "Samsung electronics unveils 6g white paper and outlines direction for ai-native and sustainable communication," https://news.samsung.com/global/samsung-electronics-unveils-6g-white-paper-and-outlines-direction-for-ai-native-and-sustainable-communication, Jun. 2023, accessed: 2025-05-06.

[2] Y. Hong, T. Thaj, and E. Viterbo, *Delay-Doppler Communications: Principles and Applications*. Academic Press, 2022.

[3] Y. Liu, M. Chen, C. Pan, T. Gong, J. Yuan, and J. Wang, "Otfs versus ofdm: Which is superior in multiuser leo satellite communications," *IEEE Journal on Selected Areas in Communications*, vol. 43, no. 1, pp. 139–151, Jan. 2025.

[4] H. Raviteja, K. T. Phan, Y. Hong, and E. Viterbo, "Interference cancellation and iterative detection for orthogonal time frequency space modulation," *IEEE Transactions on Wireless Communications*, vol. 17, no. 10, pp. 6501–6515, 2018.

[5] T. Thaj, E. Viterbo, and Y. Hong, "General i/o relations and low-complexity universal mrc detection for all otfs variants," *IEEE Access*, vol. 10, pp. 96 026–96 038, 2022.

[6] G. D. Surabhi and A. Chockalingam, "Low-complexity linear equalization for 2×2 mimo-otfs signals," in *2020 IEEE 21st International Workshop on Signal Processing Advances in Wireless Communications (SPAWC)*, 2020, pp. 1–5.

[7] P. Li, R. C. de Lamare, and R. Fa, "Multiple feedback successive interference cancellation detection for multiuser mimo systems," *IEEE Transactions on Wireless Communications*, vol. 10, no. 8, pp. 2434–2439, Aug. 2011.

[8] A. S. Bora, K. T. Phan, and Y. Hong, "Spatially correlated mimo-otfs for leo satellite communication systems," in *Proc. IEEE ICC Workshops (ICCW)*, 2022, pp. 723–728.

[9] J. Heo, S. Sung, H. Lee, I. Hwang, and D. Hong, "MIMO Satellite Communication Systems: A Survey From the PHY Layer Perspective," *IEEE Communications Surveys & Tutorials*, vol. 25, no. 3, pp. 1543–1578, 2023.

[10] R. B. Di Renna and R. C. de Lamare, "Iterative List Detection and Decoding for Massive Machine-Type Communications," *IEEE Trans. Commun.*, vol. 68, no. 10, pp. 6276–6288, 2020.

[11] 3rd Generation Partnership Project, "3rd generation partnership project; technical specification group radio access network; study on new radio (nr) to support non-terrestrial networks (release 15)," 3GPP TR 38.811 V15.3.0, Tech. Rep., Jul. 2020.

[12] ——, "3rd generation partnership project; technical specification group radio access network; study on channel model for frequencies from 0.5 to 100 ghz (release 18)," 3GPP TR 38.901 V18.0.0, Tech. Rep., Mar. 2024.